Modelling the resistive state in a transition edge sensor

A. Kozorezov,[1,a)] A. A. Golubov,[2] D. D. E. Martin,[3] P. A. J. de Korte,[4] M. A. Lindeman,[4] R. A. Hijmering,[4] J. van der Kuur,[4] H. F. C. Hoevers,[4] L. Gottardi,[4] M. Yu. Kupriyanov,[5] and J. K. Wigmore[1]

[1]*Department of Physics, Lancaster University, Lancaster, United Kingdom*
[2]*Faculty of Science and Technology and MESA+ Institute for Nanotechnology, University of Twente, Enschede, The Netherlands*
[3]*Advanced Studies and Technology Preparation Division, Scientific Projects Department, European Space Agency ESTEC, Postbus 299, Noordwijk 2200AG, The Netherlands*
[4]*SRON National Institute for Space Research, Sorbonnelaan 2, Utrecht 3584 CA, The Netherlands*
[5]*Nuclear Physics Institute, Moscow State University, Moscow 119992, Russia*

We have developed a model for the resistive transition in a transition edge sensor (TES) based on the model of a resistively and capacitively shunted junction, taking into account phase-slips of a superconducting system across the barriers of the tilted washing board potential. We obtained analytical expressions for the resistance of the TES, $R(T, I)$, and its partial logarithmic derivatives α_I and β_I as functions of temperature and current. We have shown that all the major parameters describing the resistive state of the TES are determined by the dependence on temperature of the Josephson critical current, rather than by intrinsic properties of the S-N transition. The complex impedance of a pristine TES exhibits two-pole behaviour due to its own intrinsic reactance. © *2011 American Institute of Physics*. [doi:10.1063/1.3621829]

The transition edge sensor (TES) is a simple superconducting device exhibiting unique spectroscopic capabilities for single photon detection over an energy range from near infrared to hard X-rays.[1] In spite of rapid technological progress, the theoretical limit of TES resolution has not yet been achieved. One of the reasons is the absence of a detailed physical understanding of the resistive state of the TES. Because of its complexity, a credible microscopic model has not yet been developed, and the current description of a TES is based largely on a phenomenological approach.[2] Within this model, the TES is viewed as a variable resistor, characterised by the extremely sharp dependence of its resistance on temperature, T, through the S-N phase transition and a smooth dependence on current, I. The phenomenological theory of a TES[3] takes the TES resistance $R(T, I)$ and its partial logarithmic derivatives with respect to temperature and current $\alpha_I = \partial \ln R / \partial \ln T|_I$ and $\beta_I = \partial \ln R / \partial \ln I|_T$ as known functions. These functions are used to model the TES response. In spite of spectacular progress in developing TES technology, many important problems, especially excess noise,[2] remain unresolved, indicating that a more detailed physical understanding of the resistive transition in TES is needed.

It has recently been realised that in many superconducting devices currently being developed as sensitive detectors of radiation, the essential physics must involve an understanding of TES weak link behaviour with a correct account of the long range lateral proximity effect.[4,5] Experiments with Mo-Au transition edge sensors[4] have revealed a strong, long range lateral proximity effect even in the 290 μm square samples. In addition, the critical temperature describing the transition from superconducting to resistive state was found to be a strong function of TES size and bias current. A model based on Ginzburg-Landau (GL) theory was used in Ref. 4 to interpret the data. Long range proximity effects must also play a significant role in nano- or hot electron bolometers[6] even though in nanobolometers the coherence length may be only a few tens of nanometers.

The long range proximity effect in a TES has been studied earlier at a microscopic level using the Usadel approach.[5] This method facilitates calculation of the order parameter profile in TES, its dependence on temperature and supercurrent, and also the critical Josephson current as a function of temperature for an arbitrary length of TES and arbitrary transparency of the interfaces between leads and TES. In a typical TES, the critical temperature of the leads, T_{cL}, considerably exceeds the intrinsic critical temperature of the TES film T_c. One of the results of such a modelling is that due to the proximity effect, the order parameter remains finite throughout the resistive transition of TES, and superconductivity is not destroyed. It is, therefore, evident that the resistive transition in a laterally proximised TES is not fully determined by the properties of the S-N phase transition.

A microscopic theory of electrical transport in classical weak links has been developed for tunnel[7] and later for ScS (c indicates constriction) junctions;[8] an extensive review was given by Likharev[9] and also Golubov *et al.*[10] Nonequilibrium superconductivity effects were later modelled for several specific examples of weak links.[11,12] The most significant assumption in the latter work was that the temperature remained close to T_{cL}. With this assumption, analytical solutions were obtained for several specific cases, including long links in which the length L far exceeded the coherence length, ξ. However, the physics of transition edge sensors cannot be described within these assumptions, because the TES operate at temperatures which remain much lower than the critical temperature of the superconducting leads. This

a)Author to whom correspondence should be addressed. Electronic mail: a.kozorezov@lancaster.ac.uk.

makes a general microscopic solution extremely compli-
cated, and in this work, we do not consider the full micro-
scopic model of the resistive transition in TES. Instead, we
analyse the TES within a model of a resistively and capaci-
tively shunted junction (RCSJ) and its overdamped limit,
which has previously been used to describe many important
characteristics of weak links.[9] Formal validation of this
model for such an extended system as TES is absent,
although for the limiting case of a short bridge it can be justi-
fied as following from the microscopic model, if nonequili-
brium superconductivity effects are neglected.[11] In this
work, we take the RCSJ as the simplest model incorporating
weak link behaviour in order to analyse the resistive transi-
tion in a TES. We sacrifice such nonequilibrium effects as
branch imbalance generation and relaxation, Andreev reflec-
tions, and conversion from supercurrent to normal current in
favour of model simplicity.

The expression for $R(T, I)$ in an overdamped junction
with thermal fluctuations can be obtained from the I-V char-
acteristics.[13,14] We may write[15]

$$R \equiv R(T, I) = R_N \left\{ 1 + \frac{1}{x} \text{Im} \left[\frac{I_{1+i\gamma x}(\gamma)}{I_{i\gamma x}(\gamma)} \right] \right\}. \quad (1)$$

Here, R_N is the normal state resistance, $\gamma = (\hbar I_c(T, L))/(2eT)$
is the ratio of the Josephson coupling to thermal energy,
$x = I/(I_c(T, L))$, $I_c(T, L)$ is the critical Josephson current, and
$I_{1+i\gamma x}(z)$ and $I_{i\gamma x}(z)$ are the modified Bessel functions $I_\nu(z)$ of
the complex order, ν, and real variable, z. Performing differ-
entiations, we obtain α_I and β_I,

$$\alpha_I = -\frac{\gamma}{x} \frac{d\ln I_c}{d\ln T} \frac{R_N}{R} \text{Im} \left\{ \frac{I_{-1+i\gamma x}(\gamma) I_{1+i\gamma x}(\gamma)}{I_{i\gamma x}^2(\gamma)} \right\}, \quad (2)$$

$$\beta_I = -1 + \frac{R_N}{R} \left\{ 1 - 2\text{Re} \left[I_{i\gamma x}^{-2}(\gamma) \times \int_0^\gamma dz I_{i\gamma x}(z) I_{1+i\gamma x}(z) \right] \right\}. \quad (3)$$

The entities, R, α_I, and β_I, are all functions of T and I.

With the transition temperature of the leads being typi-
cally an order of magnitude higher than the operating tem-
perature, modelling with the use of the GL theory can be
justified only for the case of a strong interfacial resistance,
leading to less than 1% electron transmission across the
interface. Even in this situation, the GL description will be
more reliable for a larger size TES, losing its applicability
closer to the leads/TES interface. To model the lateral prox-
imity effect without any limitations, we use the Usadel for-
malism and calculate the dependence of the critical
Josephson current on temperature numerically. We show the
results for the two extreme situations—strong lateral proxim-
ity effect (fully transparent lead/TES interface) and weak lat-
eral proximity effect (high interfacial resistance). Fig. 1
shows examples of the $R(T, I)$, α_I, and β_I for a typical, later-
ally proximised TES.

The RCSJ model allows us to generalise the response of
a TES to an alternating current. If the description as an over-
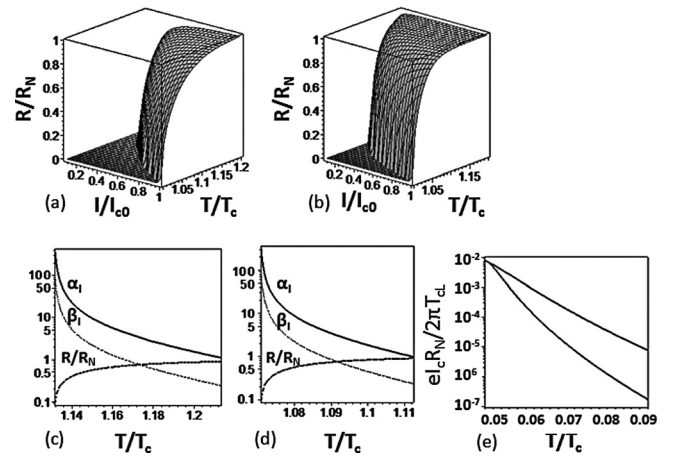damped junction is correct, then it possesses its own intrinsic

FIG. 1. (a) R(T,I) for a TES with transparent lead/TES interface; (c)
dependences of α_I, β_I, and R calculated at fixed current $I = 0.3 I_{c0}$ on temper-
ature in the range, corresponding to $0.1 \leq R/R_N \leq 0.9$: $T_{cL}/T_c = 20$, $L/\xi_N = 25$. T_c and ξ_N are TES intrinsic critical temperature and coherence
length, respectively, and $I_{c0} \equiv I_c(T_c)$; (b)-(d) as (a)-(c) but for low interface
transparency; (e) calculated critical current dependence on temperature:
upper curve—high and lower curve—low interface transparency.

reactance. The latter arises because of regular phase slippage
by 2π with characteristic frequency τ^{-1}, where
$\tau = (\hbar/2e)^2/R_N T$ is the average time a "particle" takes to
diffuse one period of a tilted washing board potential.[13,14]
The intrinsic impedance $Z_0(\omega, T, I)$ is written in terms of
Bessel functions,[15]

$$\frac{Z_0(T, I, \omega)}{R_N} = 1 - \frac{\gamma}{2} \left[\frac{I_{1+i\gamma x}(\gamma)}{I_{i\gamma x}(\gamma)(\lambda + i\omega\tau)} + \frac{I_{1-i\gamma x}(\gamma)}{I_{-i\gamma x}(\gamma)(\lambda^* + i\omega\tau)} \right], \quad (4)$$

where the expression for the eigenvalue λ is $\lambda = (\gamma I_{i\gamma x}(\gamma) I_{1+i\gamma x}(\gamma))/(2\int_0^\gamma dz I_{i\gamma x}(z) I_{1+i\gamma x}(z))$. We analyse the electric
equivalent circuit in which the variable resistor, representing
the TES, is replaced by an overdamped junction, shown in
Fig. 2(a), and solve the small signal equations[16] for the sim-
plest case of a pristine TES, with no extra electrode struc-
ture, absorber, or membrane contributing to thermal
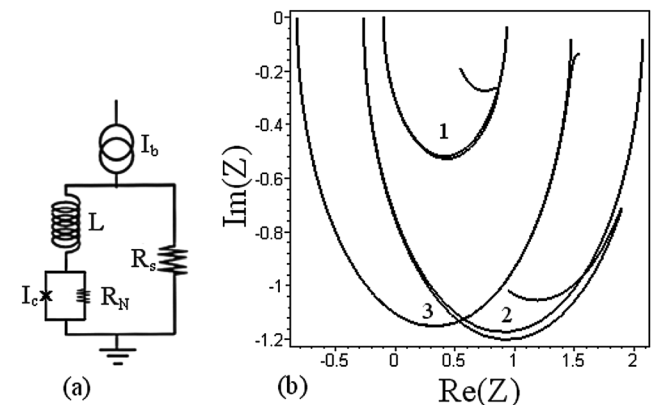decoupling. We obtain

FIG. 2. (a) Electrical equivalent circuit with the TES modelled as an over-
damped junction, $R_s \ll R$ is the shunt resistor; (b) low current complex im-
pedance with (bottom curves of the pairs) and without (top curves) account
taken of the intrinsic TES reactance: 1—$R/R_N = 0.03$, 2—$R/R_N = 0.1$, 3—$R/R_N = 0.5$.

$$Z_{TES}(\omega) = \frac{\pounds_0 R + Z_0(\omega)(1 + i\omega\tau_0)}{(1 - \pounds_0)(1 - i\omega\tau_{eff})}$$

$$= Z_{TES}^0(\omega) + \frac{1}{1 - \pounds_0} \frac{(Z_0(\omega) - Z_0(0))(1 + i\omega\tau_0)}{1 - i\omega\tau_{eff}}.$$

$$(5)$$

Here, $Z_{TES}^0(\omega) = (R(1 + \beta_I + \pounds_0)(1 + i\omega\tau_{fall}))/((1 - \pounds_0)(1 - i\omega\tau_{eff}))$ is the standard expression for the complex impedance of the TES without thermal decoupling, $\pounds_0$ is the loop gain, τ_0 is the natural (without feedback) time constant, $\tau_{eff} = \tau_0/(\pounds_0 - 1)$, and $\tau_{fall} = \tau_0/[1 + \pounds_0/(1 + \beta_I)]$. Fig. 2(b) shows the calculated impedance at a constant TES current at different temperatures, illustrating the effect of the second higher frequency pole. The numbers are chosen for illustrative purposes only and the curves sequence does not reflect any experiment imposing specific constraints on TES temperature, current, or bath temperature. It is seen that, as expected, the contribution of intrinsic reactance (the difference between the top and bottom curves of the pairs in Fig. 2) is greater for lower values of the ratio R/R_N, lessening with increasing of the normal current. At $R/R_N = 0.1$, the effect of including the intrinsic reactance of the TES may become observable already at $\omega\tau \simeq 1$. For $R_N = 20$ mΩ and $T = 100$ mK, this falls into frequency range $f \geq 50$ kHz. However, the cusp, where Im$Z_{TES}(\omega) = 0$ (both inward and outward inflexions of the complex impedance curve are possible for different TES parameters) can only be seen for $\omega\tau \geq 1$ (typically $\omega\tau \gg 1$), depending on the exact values of $\pounds_0$, τ_0, τ_{eff}, and τ. Thus, observation of the two pole behaviour and cusp in the frequency range up to 1 MHz of a pristine TES without any thermal decoupling would serve as direct evidence of the intrinsic reactance of the TES and would also support the RCSJ model of its resistive state. This contribution can easily be separated from any stray dangling heat capacity. Indeed, as seen from Fig. 2, since the second pole contribution is of electronic origin, it changes rapidly across the narrow resistive transition range. No other thermally decoupled subsystem would exhibit this behaviour. Finally, we note that an observable effect of the second pole at lower frequencies $\omega\tau \geq 1$ occurs in the relatively narrow region of (T,I) phase space, at small currents, for which calculations leading to results in Fig. 2(b) were made. For large bias currents, the Josephson coupling energy is large in comparison with $k_b T$, so that the complex impedance over a broad frequency range approaches the classical result, and the two-pole behaviour can only be detected at high frequencies $\omega\tau \gg 1$.

In summary, we have shown that the RCSJ model can provide a realistic description of the resistive state of a transition edge sensor. The model predicts the specific contribution to the complex impedance of a TES due to its intrinsic reactance. Observation of this frequency dependence and a quantitative analysis of dedicated experiments are important for further validation of the RCSJ approach.

[1]A. S. Hoover, M. K. Bacrania, N. J. Hoteling, P. J. Karpius, M. W. Rabin, C. R. Rudy, D. T. Vo, J. A. Beall, D. A. Bennett, W. B. Doriese, G. C. Hilton, R. D. Horansky, K. D. Irwin, J. N. Ullom, and L. R. Vale, J. Radioanal. Nucl. Chem. **282**, 227 (2009).

[2]K. D. Irwin, G. C. Hilton, in *Topics in Applied Physics*: "Cryogenic particle detection," edited by C. Enss, (Springer, Berlin, 2005).

[3]K. D. Irwin, Appl. Phys. Lett. **66**, 1998 (1995).

[4]J. E. Sadleir, S. J. Smith, S. R. Bandler, J. A. Chervenak, and J. R. Clem, Phys. Rev. Lett. **104**, 047003 (2010).

[5]A. G. Kozorezov, A. A. Golubov, D. D. Martin, P. deKorte, M. Lindeman, R. Hijmering, and J. K. Wigmore, IEEE Trans. Appl. Supercond. **21**, 250 (2011).

[6]J. Wei, D. Olaya, B. S. Karasik, S. V. Pereverzev, A. V. Sergeev, and M. E. Gershenzon, Nat. Nanotechnol. **3**, 496 (2008).

[7]N. R. Werthamer, Phys. Rev. **147**, 255 (1966).

[8]L. G. Aslamazov and A. I. Larkin, JETP Lett. **9**, 87 (1969).

[9]K. K. Likharev, Rev. Mod. Phys. **51**, 101 (1979).

[10]A. A. Golubov, M. Yu. Kupriyanov, and E. Ilichev, Rev. Mod. Phys. **76**, 411 (2004).

[11]S. N. Artemenko and A. F. Volkov, Usp. Fiz. Nauk **128**, 4 (1979).

[12]L. G. Aslamazov, A. F. Volkov, in *Nonequilibrium Superconductivity* edited by D. N. Langenberg and A. I. Larkin (Elsevier, Amsterdam, 1986).

[13]Yu. M. Ivanchenko and L. A. Zilberman, Sov. Phys. JETP **28**, 1272 (1969).

[14]V. Ambegaokar and B. I. Halperin, Phys. Rev. Lett. **22**, 1364 (1969).

[15]W. T. Coffey, Y. P. Kalmykov, S. V. Titov, and L. Cleary, Phys. Rev. E **78**, 031114 (2008).

[16]M. A. Lindeman, S. Bandler, R. P. Brekosky, J. A. Chervenak, E. Figueroa-Feliciano, F. Finkbeiner, M. J. Li, and C. A. Kilbourne, Rev. Sci. Instrum. **75**, 1283 (2004).